

A transistor-based biosensor for the extraction of physical properties from biomolecules

Sungho Kim, David Baek, Jee-Yeon Kim, Sung-Jin Choi, Myeong-Lok Seol et al.

Citation: *Appl. Phys. Lett.* **101**, 073703 (2012); doi: 10.1063/1.4745769

View online: <http://dx.doi.org/10.1063/1.4745769>

View Table of Contents: <http://apl.aip.org/resource/1/APPLAB/v101/i7>

Published by the [American Institute of Physics](http://www.aip.org).

Related Articles

Light emission and current rectification in a molecular device: Experiment and theory
J. Appl. Phys. **112**, 113108 (2012)

Rectifying and perfect spin filtering behavior realized by tailoring graphene nanoribbons
J. Appl. Phys. **112**, 114319 (2012)

Spin filter and molecular switch based on bowtie-shaped graphene nanoflake
J. Appl. Phys. **112**, 104328 (2012)

Universal scaling of resistivity in bilayer graphene
Appl. Phys. Lett. **101**, 223111 (2012)

Charge redistribution in a charge storage layer containing C60 molecules and organic polymers for long electron retention
APL: Org. Electron. Photonics **5**, 252 (2012)

Additional information on *Appl. Phys. Lett.*

Journal Homepage: <http://apl.aip.org/>

Journal Information: http://apl.aip.org/about/about_the_journal

Top downloads: http://apl.aip.org/features/most_downloaded

Information for Authors: <http://apl.aip.org/authors>

ADVERTISEMENT

AIP | Applied Physics
Letters

SURFACES AND INTERFACES
Focusing on physical, chemical, biological, structural, optical, magnetic and electrical properties of surfaces and interfaces, and more...

ENERGY CONVERSION AND STORAGE
Focusing on all aspects of static and dynamic energy conversion, energy storage, photovoltaics, solar fuels, batteries, capacitors, thermoelectrics, and more...

EXPLORE WHAT'S NEW IN APL

SUBMIT YOUR PAPER NOW!

A transistor-based biosensor for the extraction of physical properties from biomolecules

Sungho Kim, David Baek, Jee-Yeon Kim, Sung-Jin Choi, Myeong-Lok Seol, and Yang-Kyu Choi^{a)}

Department of Electrical Engineering, KAIST, 291 Daehak-ro, Yuseong-gu, Daejeon, 305-701, South Korea

(Received 4 April 2012; accepted 26 July 2012; published online 14 August 2012)

An analytical technique is proposed that uses an asymmetric double-gate field-effect transistor (FET) structure to characterize the electrical properties of biomolecules, including their permittivity and charge density. Using a simple measurement with the proposed FET structure, we are able to extract the physical properties (i.e., permittivity and charge density) of biomolecules. A reliable analytical tool for the characterization of biomolecules can be provided by the proposed FET structure without a complex measurement system. It is expected that the proposed method will be expanded into a universal analysis technique for the electrical evaluation of biomolecules in applications beyond biosensing. © 2012 American Institute of Physics. [<http://dx.doi.org/10.1063/1.4745769>]

The electronic detection of biomolecules using various nanostructures has attracted a great deal of attention in the last 10 years. This technique has become viewed as a feasible application as a result of the development and fusion of bio- and nanotechnologies.¹ Owing to the fast, low-cost, and high-throughput analysis capability of biological processes, systems based on nanosensor arrays promise to revolutionize many areas in medicine and biochemistry, ranging from the detection and diagnosis of diseases to the discovery of drug delivery systems.

Thus far, biosensor applications capable of diagnosing disease have been successfully demonstrated, particularly when they have been based on the nanowire transistor structure. A very high level of sensitivity, detectable below the fM regime, has been achieved, and an analysis of its mechanism has been clearly developed.² In contrast, research into electrical characterizations capable of evaluating the physical properties of biomolecules remains in its infancy. Most previous reports have utilized massive and complicated optical systems to measure the thickness and refractive index of biomolecules.³ Others have used demanding numerical simulation techniques to determine the amount of charge inside a biomolecule.⁴ In addition, previous characterization methods have not been optimized for the detection of the specific binding of biomolecules, thus leading to a low sensitivity for biosensing.⁵

In this work, an analytical technique is proposed for the characterization of the physical properties of biomolecules, specifically, the permittivity and charge density. With an asymmetric double-gate transistor structure, the physical properties and the specific binding of the biomolecules can be monitored through this simple measurement technique. Consequently, both biosensing and the electrical characterization of biomolecules can be carried out in a single test device, demonstrating the potential for an all-in-one type of analytical methodology.

^{a)}Author to whom correspondence should be addressed. Electronic mail: ykchoi@ee.kaist.ac.kr. Tel.: +82-42-350-3477.

Figure 1(a) shows a schematic of the asymmetric double-gate transistor composed of a Si nanowire (Si-NW). One notable feature of the proposed structure is its asymmetric gate dielectric layer. As shown in Fig. 1(a), the gate dielectric between gate-1 ($G1$) and the Si-NW is composed of a thin oxide (t_{oxf}). In contrast, the gate dielectric on the

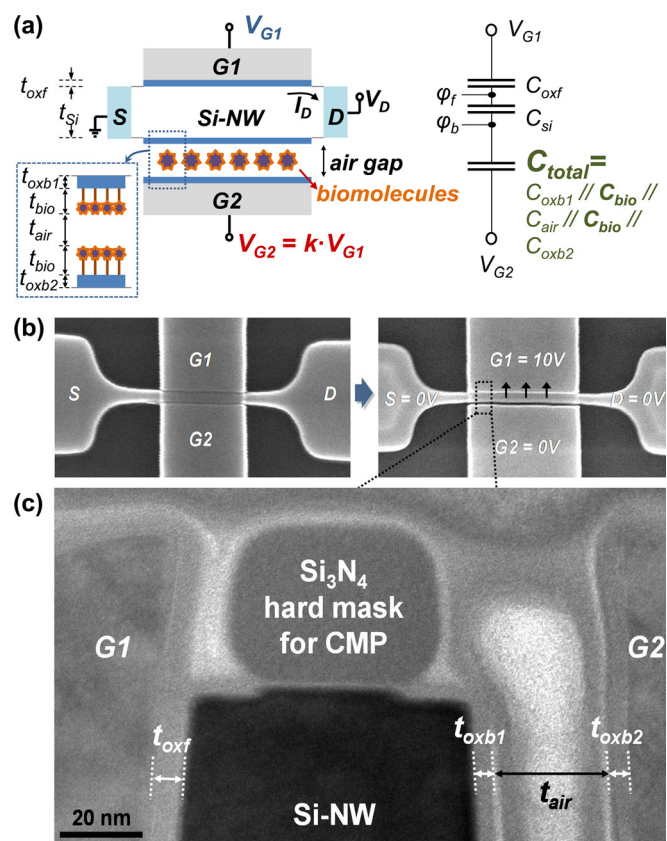


FIG. 1. (a) Schematic of the proposed asymmetric double-gate transistor structure. The open-air gap between $G2$ and the Si-NW serves as the location for the immobilization of the biomolecules. (b) SEM images of an asymmetric double-gate transistor. After the bias ($V_{G1} = 10\text{ V}$) is applied, the Si-NW adheres to $G1$. (c) A TEM image after the attachment of Si-NW to $G1$.

opposite side, between gate-2 ($G2$) and the Si-NW, is composed of an air gap in which targeted biomolecules are immobilized. Thus, by monitoring the change in the drain current (I_D) before and after the immobilization of the biomolecules, the physical properties (permittivity and charge density) and the specific binding of the biomolecules can be characterized.

The double-gate transistor structure is composed of an asymmetric gate dielectric layer and was realized with the implementation of a mechanically bendable device known as a fin flip-flop actuated channel transistor (FinFACT).⁶ A p-type (100) silicon-on-insulator (SOI) substrate with a top silicon thickness of 100 nm was used as a starting material. Boron ions ($N_a = 10^{18} \text{ cm}^{-3}$) were implanted into the silicon layer. A Si-NW with a width of 40 nm was patterned with the aid of a nitride hard mask. An oxide layer with a thickness of 20 nm was conformally deposited over the Si-NW as a sacrificial layer, followed by the *in-situ* deposition of an n⁺ polycrystalline silicon (poly-Si) layer for the gate electrode. The poly-Si gate was then separated by a chemical-mechanical polishing (CMP) step. The two separated gate electrodes were placed on both sides of the Si-NW. Each gate can control the current-voltage characteristics independently. After the gate electrode was patterned (the nominal gate length used for these experiments was 500 nm), source/drain (S/D) ion implantation using phosphorus was carried out. The sacrificial oxide was then removed using a dilute HF solution, and the buried oxide (BOX) beneath the Si-NW was simultaneously etched. At this point, the suspended Si-NW was anchored at both ends, i.e., the pads for the source and the drain probing. When the Si-NW was floating in the air, it was movable and bendable. The exposed surfaces of the Si-NW and the gate were reoxidized with a 5-nm-thick oxide. The Si-NW was forced to adhere to $G1$ by applying a voltage ($V_{G1} = 10 \text{ V}$, $V_S = V_D = V_{G2} = 0 \text{ V}$) to it, as shown in Fig. 1(b). Thus, the gate dielectric between $G1$ and the Si-NW was entirely composed of the oxide. In contrast, the gate dielectric between $G2$ and the Si-NW was composed of an air gap and the oxide. This air gap functions as the immobilization location for the targeted biomolecules. Finally, annealing was carried out under a forming gas ($\text{N}_2:\text{H}_2 = 9:1$) atmosphere at 450°C to remove interface defects.

To measure the permittivity of targeted biomolecules using the asymmetric double-gate transistor, the subthreshold slope (SS) characteristic governed by the rate of gate bias sweeping was investigated. This technique involves simultaneously sweeping a voltage, V_{G1} for gate $G1$ and V_{G2} for gate $G2$, while maintaining a constant gate bias ratio, k ($\equiv V_{G2}/V_{G1}$). In the fully depleted (FD) SOI film, the corresponding potentials at the front and back interface, ϕ_f and ϕ_b , respectively, are related to V_{G1} and V_{G2} as follows:⁷

$$V_{G1} = V_{FB1} + \left(1 + \frac{C_{Si} + C_{if}}{C_{oxf}}\right) \phi_f - \frac{C_{Si}}{C_{oxf}} \phi_b - \frac{Q_d/2}{C_{ox}}, \quad (1)$$

$$V_{G2} = V_{FB2} + \frac{Q_{bio}}{C_{total}} - \frac{C_{Si}}{C_{total}} \phi_f + \left(1 + \frac{C_{Si} + C_{itb}}{C_{total}}\right) \phi_b - \frac{Q_d/2}{C_{total}}. \quad (2)$$

Here, the following variables are defined. $Q_d = -qN_a t_{Si}$ is the depletion charge, Q_{bio} is the additional charge density from the biomolecules, C_{Si} is the silicon depletion capacitance, C_{oxf} is the capacitance between $G1$ and the channel, $C_{total} = C_{oxb1}/C_{bio}/C_{air}/C_{bio}/C_{oxb2}$ is the total capacitance between $G2$ and the channel, C_{if} and C_{itb} are the interface trap capacitance at the front and back interfaces of the SOI films, respectively, ϕ_f and ϕ_b are the surface potential at the front and back interfaces of the SOI films, respectively, and V_{FB1} and V_{FB2} are the corresponding front and back channel flatband voltage.

Because $V_{G2} = k \cdot V_{G1}$ under double-gate operation, the respective rate of increase in ϕ_f and ϕ_b can be expressed as follows:

$$\frac{d\phi_f}{dV_{G1}} = \frac{C_{oxf}(C_{Si} + C_{bio} + C_{itb}) + kC_{bio}C_{Si}}{(C_{Si} + C_{oxf} + C_{if})(C_{Si} + C_{bio} + C_{itb}) - C_{Si}^2}, \quad (3)$$

$$\frac{d\phi_b}{dV_{G2}} = \frac{kC_{bio}(C_{Si} + C_{bio} + C_{if}) + C_{oxf}C_{Si}}{(C_{Si} + C_{oxf} + C_{if})(C_{Si} + C_{bio} + C_{itb}) - C_{Si}^2}. \quad (4)$$

As a consequence of the capacitive coupling between the front and back interfaces in the FD SOI film, the change in ϕ_f can significantly influence the change in ϕ_b . An optimum coupling condition occurs when both surface potentials increase at the same rate with respect to the applied front gate voltage, i.e., when $d\phi_f/dV_{G1} = d\phi_b/dV_{G2}$. Setting Eqs. (3) and (4) equal to each other yields the corresponding optimum gate bias ratio, k_o , which is given as

$$k_o = \frac{C_{oxf}(C_{total} + C_{itb})}{C_{total}(C_{oxf} + C_{if})} \approx 1 + \frac{C_{itb}}{C_{total}}. \quad (5)$$

The approximation made in Eq. (5) is valid if the front gate dielectric is sufficiently thin, such that $C_{oxf} \gg C_{if}$. Because the front gate dielectric thickness (t_{oxf}) is less than 10 nm, as shown in Fig. 1(c), this assumption is valid.

To determine k_o experimentally, the SS of the FD SOI MOSFET under double-gate operation was investigated. In actuality, the subthreshold slope at the point of optimum coupling during double-gate operation has been previously determined⁸

$$SS = \ln(10) \cdot \left(1 + \frac{C_{if}}{C_{oxf}}\right). \quad (6)$$

This is approximately 60 mV/dec at room temperature because $C_{oxf} \gg C_{if}$. Therefore, by plotting the measured subthreshold slope values according to k , the value that corresponds to 60 mV/dec is k_o . Subsequently, C_{total} can be calculated from Eq. (5) and the well-known value of the interface trap density ($C_{itb} = q^2 \cdot D_{itb}$, $D_{itb} = 10^{10} \text{ cm}^{-2} \text{ eV}$). As shown in Fig. 1(a), C_{total} consists of a series of five different capacitances, $C_{total} = C_{oxb1}/C_{bio}/C_{air}/C_{bio}/C_{oxb2}$. Consequently, if the thickness of the biomolecules (t_{bio}) is known with precision, the permittivity of the biomolecules (ϵ_{bio}) can be extracted by $C_{bio} (= \epsilon_{bio}/t_{bio})$.

In addition, the relationship between V_{G2} and the threshold voltage (V_T) was determined as shown below.⁷

$$\frac{dV_T}{dV_{G2}} = \frac{dV_T}{dQ_{bio}} \frac{dQ_{bio}}{dV_{G2}} = -\frac{C_{Si}C_{total}}{C_{oxf}(C_{Si} + C_{total})}. \quad (7)$$

Using $dQ_{bio}/dV_{G2} = C_{total}$ from Eq. (2), this can be obtained as follows:

$$\Delta V_T = -\frac{C_{Si}}{C_{oxf}(C_{Si} + C_{total})} \Delta Q_{bio}. \quad (8)$$

As a result, from the measured difference of V_T (ΔV_T) and the extracted C_{total} value, the charge density of the biomolecules (Q_{bio}) can be calculated.

Prior to the bio-experiments, the asymmetric double-gate transistor with the air gap was cleaned thoroughly with deionized water (DW) and dried in a stream of high-purity nitrogen. The cleaned device was then placed in a 1% (v/v) solution of 3-aminopropyltriethoxysilane (APTES, Sigma) in ethanol for 30 min, rinsed five times in ethanol, and dried at 120 °C for 10 min. The device, which had an amino-functionalized surface, was subsequently immersed in a sulpho-NHS-LC-biotin (Pierce) solution for 1 h, which had been dissolved in a phosphate-buffered saline solution (PBS, Sigma-Aldrich). The concentration was adjusted to 10 mM. The device was then washed with DW and PBS to remove any unreacted residual molecules from the surface. The biotinylated device was then immediately immersed into a streptavidin/PBS solution for another hour, followed by washing with DW and blow-drying in nitrogen.

Figure 2 shows the measured drain current-gate voltage (I_D - V_{G1}) characteristics before and after the bio-experiments when $k = 1$ ($V_{G1} = V_{G2}$). Two distinctive characteristics were revealed after the bio-experiments. First, the subthreshold slope steepened after immobilization of the biomolecules inside the air gap. This occurred due to an increase in C_{total} as a consequence of a permittivity increase from ϵ_{air} to ϵ_{bio} caused by the biomolecules. Second, the curve shifted to the right-hand side after the bio-experiments. This was due to a combination of both the additional charge (Q_{bio}) included in the biomolecules and the increase in permittivity

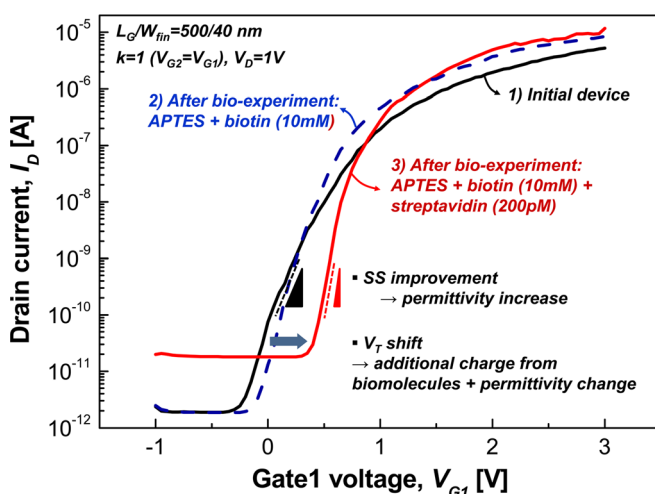


FIG. 2. The measured drain current-gate voltage (I_D - V_{G1}) characteristics before and after the bio-experiments for the condition of $k = 1$ ($V_{G1} = V_{G2}$). The steepened subthreshold slope and shifted threshold voltage provide the information about ϵ_{bio} and Q_{bio} .

(an analogy can be seen in Eq. (8), where ΔV_T is affected by both C_{total} and Q_{bio}). It is known that APTES has positive charges in solution at a neutral pH.⁹ Because all bio-reagent solutions were prepared and adjusted to pH 7.4 using PBS, APTES was positively charged in the present experiment. In contrast, biotin (pI = 3.5) and streptavidin (pI = 5–6) were negatively charged, as their pI values were lower than that of PBS.^{1,10} Accordingly, the net charge polarity of the APTES + biotin + streptavidin bindings is expected to be negative, and the predicted charge of ΔV_T is positive, which is consistent with the shift in direction of the measured curve, as shown in Fig. 2.

The effects arising from the permittivity change and Q_{bio} are not separately analyzed from simple I_D - V_{G1} characteristics because these effects are coupled together. This can be one of the constraints in conventional FET-based biosensors. In other words, both effects can lead to changing the I_D - V_{G1} characteristic simultaneously. Therefore, it is not possible to determine which effect is dominant. When a FET is used for a biosensor application, the coupling issue is no longer a concern, even though other information cannot be obtained from simple ΔI_D characteristics. With the proposed technique, these effects can be investigated individually and quantitatively. To measure the effect of the permittivity change quantitatively, regardless of Q_{bio} (to extract the permittivity of the biomolecules (ϵ_{bio}) experimentally), Fig. 3 shows the measured SS values dependent on different gate bias ratios, k ($= V_{G2}/V_{G1}$). As mentioned earlier, the subthreshold slope reaches 60 mV/dec when an optimum coupling is made between $d\phi_f/dV_{G1}$ and $d\phi_b/dV_{G2}$. From the measured optimum gate bias ratio (k_o) and according to Eq. (5), C_{total} and, consequently, ϵ_{bio} ($= C_{bio} \cdot t_{bio}$) can be extracted.

To confirm the validity of the proposed technique, an initial device with only an air gap was tested. As shown in Fig. 3, the measured optimum gate bias ratio was 3.5, and the extracted permittivity of air was 1.15, showing good agreement with the known values (the ideal value of ϵ_{air} is 1).

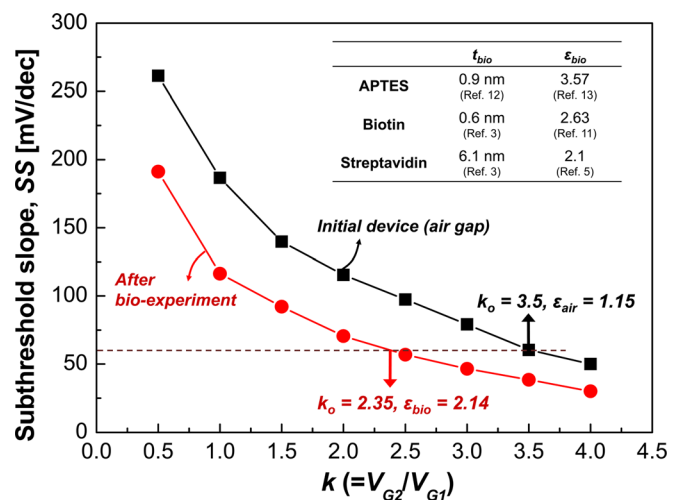


FIG. 3. The measured subthreshold slope values depending on the different gate bias ratios of k ($= V_{G2}/V_{G1}$). ϵ_{bio} can be extracted from the point where the subthreshold slope reaches 60 mV/dec. The inset table summarizes the reported permittivity and thickness values for APTES, biotin, and streptavidin.

Therefore, the validity of the proposed technique is guaranteed for the extraction of the permittivity. Next, the same measurement was carried out after the immobilization of the biomolecules (APTES + biotin + streptavidin) in the air gap. Because streptavidin is thicker than the others, as summarized in the inset table of Fig. 3, the overall capacitance of the biomolecules (C_{bio}) is primarily determined by the permittivity of streptavidin. In Fig. 3, the measured value of k_o after the bio-experiment changed from 3.5 to 2.35, and the extracted permittivity was found to be 2.14, which is in good agreement with reported values of streptavidin from optical measurements.^{5,11-14} Figure 4 shows an additional verification of the proposed technique using a three-dimensional (3-D) numerical device simulation.¹⁵ As shown in Fig. 4, the measured subthreshold slope characteristics occurring due to the different gate bias ratios matches that of the simulation results well, serving as an alternative confirmation of the validity of the proposed analytical technique.

Additionally, the total charge density of the biomolecules (Q_{bio}) was calculated to be -4.48×10^{-17} coulomb/cm², or approximately 280 electrons/cm², from the measured value of $\Delta V_T = 0.45$ V with 200 pM of streptavidin, according to Eq. (8). Unfortunately, quantitatively calculated charge density values for biotin-streptavidin bindings have not been reported in the literature. Therefore, a comparative analysis of the extracted value of Q_{bio} is not available; there is a need for further verification by other methods.

In summary, the proposed technique was able to extract the permittivity (ϵ_{bio}) and charge density (Q_{bio}) of biomolecules electrically without the use of a complicated measurement system. In addition, this technique was able to clearly differentiate the effect of the permittivity change from that of an additional charge, permitting a quantitative analysis of the biosensing mechanism. Moreover, the specific binding between biomolecules was also detectable by measuring ΔV_T . Thus, the application of the proposed technique can be expanded to an all-in-one analysis technique for the evaluation of the physical properties of biomolecules in applications beyond biosensing.

This work was supported by the Center for Integrated Smart Sensors funded by the Ministry of Education, Science and Technology as Global Frontier Project (CISS-2011-0031845) and the National Research and Development

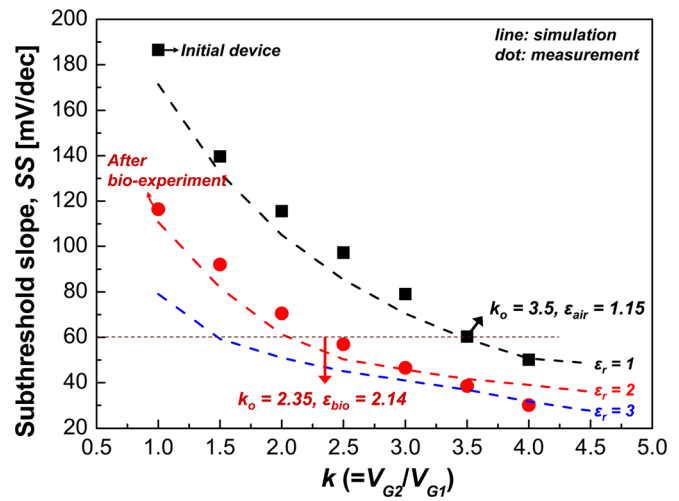


FIG. 4. 3-D device simulation results to confirm the validity of the proposed technique. The measured subthreshold slope data are consistent with the simulation results.

Program (NRDP, 2012-0001131) for the development of biomedical function monitoring biosensors.

- ¹Y. Cui, Q. Wei, H. Park, and C. M. Lieber, *Science* **293**, 1289 (2001).
- ²X. P. A. Gao, G. Zheng, and C. M. Lieber, *Nano Lett.* **10**, 547 (2010).
- ³G. H. Cross, A. A. Reeves, S. Brand, J. F. Popplewell, L. L. Peel, M. J. Swann, and N. J. Freeman, *Biosens. Bioelectron.* **19**, 383 (2003).
- ⁴M. Barbaro, A. Bonfiglio, and L. Raffo, *IEEE Trans. Electron Devices* **53**, 158 (2006).
- ⁵S. Busse, V. Scheumann, B. Menges, and S. Mittler, *Biosens. Bioelectron.* **17**, 704 (2002).
- ⁶J.-W. Han, J.-H. Ahn, and Y.-K. Choi, *IEEE Electron Device Lett.* **31**, 764 (2010).
- ⁷H.-K. Lim and J. G. Fossum, *IEEE Trans. Electron Dev.* **ED-30**, 1244 (1983).
- ⁸D. J. Wouters, J. P. Colinge, and H. E. Maes, *IEEE Trans. Electron Devices* **37**, 2022 (1990).
- ⁹M. Bezanilla, S. Manne, D. E. Laney, Y. L. Lyubchenko, and H. G. Hansma, *Langmuir* **11**, 655 (1995).
- ¹⁰S. Ghafouri and M. Thompson, *Langmuir* **15**, 564 (1999).
- ¹¹A. Densmore, D. X. Xu, S. Janz, P. Waldron, T. Mischki, G. Lopinski, A. Delage, J. Lapointe, P. Cheben, B. Lamontagne, and H. H. Schmid, *Opt. Lett.* **33**, 596 (2008).
- ¹²H.-J. Kim, S. M. Jung, Y.-H. Kim, B.-J. Kim, S. Ha, Y.-S. Kim, T.-S. Yoon, and H. H. Lee, *Thin Solid Films* **519**, 6140 (2011).
- ¹³E. Makarona, E. Kapetanakis, D. M. Velessiotis, A. Douvas, P. Argitis, P. Normand, T. Gotszalk, M. Woszczyna, and N. Glezos, *Microelectron. Eng.* **85**, 1399 (2008).
- ¹⁴H. Morgan, D. M. Taylor, and C. D'Silva, *Thin Solid Films* **209**, 122 (1992).
- ¹⁵Silvaco Int., ATLAS User's Manual, Santa Clara, CA, 2009.